Research Article Vol. 3, No. 10 / 15 October 2020 / OSA Continuum 2808

OSA CONTINUUM

Maskless lithography for versatile and low cost fabrication of polymer based micro optical structures

MUHAMMAD SHAUKAT KHAN,[1,*] ROLAND LACHMAYER,[2,3] AND BERNHARD ROTH[1,3]

[1] Hannover Centre for Optical Technologies, Leibniz University Hannover, 30167 Hannover, Germany
[2] Institut für Produktentwicklung und Gerätebau, Leibniz University Hannover, 30167 Hannover, Germany
[3] Cluster of Excellence PhoenixD, Leibniz University Hannover, 30167 Hannover, Germany
[*] Muhammad.khan@hot.uni-hannover.de

Abstract: For applications in optical communication, sensing or information projection in automotive lighting, polymer based optical devices are of keen interest. Optical structures such as waveguides and gratings are basic blocks for these devices. We report on a simple, versatile, and yet low-cost fabrication method suited for both binary and multilevel diffractive microstructures as well as multimode optical waveguides in polymers. The fabrication of the diffractive structures, i.e. gratings, with two and multiple levels, is achieved by using a maskless optical lithography system employing a spatial light modulator. With the same system, waveguide cladding structures are realized by stitching of multiple single exposure patterns. For replication of these structures on polymer, e.g. polymethyl methacrylate (PMMA), a lab-made hot embossing machine is used. We then employ UV curable material and doctor blading to realize the waveguide cores. The created diffractive and waveguide structures are characterized in terms of diffraction efficiency and optical propagation loss, respectively, showing good optical quality and performance. With our fabrication system we have demonstrated a diffraction efficiency of 71% for multilevel grating structure and a propagation loss for stitched waveguides of 2.07 dB/cm at a wavelength of 638 nm. These basic elements will be employed to realize entire optical measurement systems for applications in sensing and integrated photonics in the next step.

1. Introduction

Polymer based optical devices containing microstructures in the sub-micron range are of keen interest for applications in illumination and sensing as well as for optical interconnects [1–4]. Polymer materials for fabrication of optical devices have commonly been employed due to their high transmission efficiency, good stability, and low cost [5]. The fabrication of diffractive microstructures and waveguides on polymers i.e. PMMA (polymethyl methacrylate) can be of interest for applications such as information projection in automotive lighting [6], or for sensing [7]. The challenging task is to fabricate structures with submicron periods and depths at a high speed and low cost. Multiple methods for fabrication of microstructures on polymers have been used so far, e.g. direct laser writing DLW, interference lithography and projection lithography etc. [8]. A single point-based laser processing system, where a single beam of light is focused onto the sample for writing of continuous structures has also been demonstrated [9]. The single point-based fabrication system tends to be efficient in terms of geometric flexibility, but at very low speed. Among other methods optical projection lithography proved to be efficient with respect to cost and flexibility. Optical projection lithography can be divided into two categories: maskless projection systems and systems with projection mask. An optical system

#400056 https://doi.org/10.1364/OSAC.400056
Journal © 2020 Received 15 Jun 2020; revised 29 Aug 2020; accepted 29 Aug 2020; published 29 Sep 2020

OSA CONTINUUM

with a projection mask provides less flexibility as compared to a maskless system. In maskless projection lithography, a digital micro mirror device (DMD), or a liquid crystal display spatial light modulator (LCD SLM) is used to project micro-patterns and, thus, create microstructures onto photoresist [10,11,12]. Use of DMD in combination with high numerical aperture projection lens system to fabricate microstructures has also been reported [13]. Maskless plasmonic lithography based on multi-stage plasmonic lens utilizing both propagating surface plasmons an localized surface plasmons to achieve sub-nano sizes structures has also been reported [14]. Use of double gray-scale digital maskless lithography to fabricate curved microlens array with single lens diameter of 70 μm has also been demonstrated [15]. Use of DMD based projection lithography for fabricating Dammam gratings down to 1.5 μm has also been reported [16]. The use of an LCD SLM for microstructure pattern projection on the sample, e.g. photoresist, allows not only the realization of binary level structures but also of multilevel structures in comparison to the DMD. However, using a laser source for writing microstructures in polymer, e.g. PMMA, a high intensity of incoming light might damage the liquid crystals of the SLM. In this paper, we present a versatile LCD SLM based method for reliable fabrication of both binary and multilevel microstructures as well as multimode optical waveguides on polymer material, i.e. PMMA, by combining maskless lithography and soft replication using hot embossing and doctor blading.

2. Maskless optical system

The maskless optical setup used in this work can be seen in Fig. 1. It consists of a UV LED at a wavelength of 405 nm used as illumination source. In order to fabricate the desired structures, an LCD SLM is employed to modulate the incoming light in the desired shape and project it onto the sample. The device (Holoeye, 6001) is an 8-bit modulator with a resolution of 1920×1080 pixels with each pixel having a size of 8×8 μm^2. The modulated incoming light from the SLM is demagnified through a plan-achromatic objective lens with a numerical aperture of 0.3 and a magnification of 10. A homogenous intensity distribution of the incoming light is necessary to illuminate the SLM screen for homogenous microstructure pattern on the sample. For this, a Koehler illumination system [17] is created to homogenously illuminate the SLM screen. The samples employed here are UV sensitive photoresists: a binary or electronic positive photoresist (Shipley S1813) and a grayscale positive photoresist (Ormocomp). Ormocomp resist belongs to the family of the hybrid polymers known as organically modified ceramics (Ormocers). Ormocomp is chosen because of thermal stability, low polymerization shrinkage by volume which makes it suitable for very small features. Also, its solvent free composition allows smaller bake and developer times. The photoresists are coated on a silicon wafer with a thickness of 500 μm, using a spin coating system (WS-650SX-6NPP-LITE, Laurell). The thickness of the

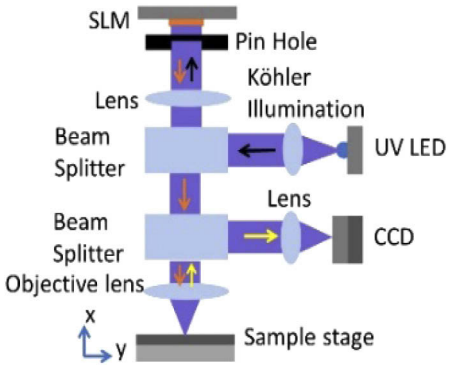

Fig. 1. The maskless optical system used for fabrication.

OSA CONTINUUM

photoresist layer is controlled by the spinning speed, which can be programmed as desired. A motorized sample stage (M-682.174, Physik Instrumente GmbH) is also included in the setup to stitch single patterns of an area of 1.32 mm^2 to a total processible area of 13.2 mm^2. Both the binary and multilevel grating structures reported, can be realized using our setup and by varying the illumination pattern. Also, single line-shaped patterns are stitched together to form a larger waveguide structure. To monitor the fabrication of the patterns on the sample a CCD camera (Pike F421b, Allied Vision) is also included in the setup. From the cost perspective, considering other standard lithographic setups with components cost ranging from 50 thousand euros and above, the optical setup presented can be implemented with standard optical and mechanical components approximately under 20 thousand euros, considering cost of spatial light modulator (LCOS SLM), objective lens, and translation stage.

3. Fabrication and replication of the optical structures

The incident UV light on the SLM screen is modulated in amplitude by displaying an image onto the SLM screen using a computer software. The image contains the shape of the desired microstructures which needs to be projected on the sample. The sample preparation is different for both photoresists used here. For the binary photoresist, the wafer is coated at a spinning speed of 4000 rpm to achieve the desired layer thickness i.e. 400 nm. The thickness of the resist is measured using a confocal microscope (Keyence VHX-7000). The resist is deposited on the surface which also has an additional uncoated region and the height difference between the two regions is measured. After exposing the resist with a desired modulated intensity from the SLM, the height profile of the grating structures is determined using the same confocal microscope. The sample is then soft baked at a temperature of 105 °C on a heating plate for 2 mins to remove any residual. To achieve the desired thickness for the grayscale photoresist, which has higher viscosity, a thinner (Ormothin) is added to the Ormocomp resist. The ratio of the Ormocomp and Ormothin is important as the layer thickness depends on the ratio of the components alongside the spinning speed. As this resist has a higher viscosity in comparison to the electronic resist, it would have to be deposited at a much higher spinning speed in order to achieve the desired layer thickness, which is well above the ability of the equipment. To overcome this, we have used a 3:1 weighted ratio of Ormocomp to Ormothin. This combination helps to realize the desired layer thickness with a lower spinning speed. The combination of photoresist and thinner is applied on the wafer and spinned at speed of 7000 rpms to achieve the required thickness i.e. 700 nm, for multilevel gratings in this case. The photoresist is then soft baked at a temperature of 80 °C for 2 mins on a hot plate. Then, the coated samples are patterned with the desired structures. For multilevel structures, the intensity is modulated in amplitude to achieve multiple heights level by displaying the grayscale image on the SLM screen.

Once the desired microstructure pattern is projected on the resists with an exposure time of 10 sec. for binary resist and 30 sec. for Ormocomp resist, the samples are then developed. For the electronic resist, we have used MF-26A developer. The sample is placed in the developer for 2 mins followed by a bath with isopropanol and distilled water and drying using pressurized air. For grayscale photoresists, the sample is cured at 115 °C on a hot plate for 10 mins to fully crosslink the exposed area to the wafer and after that, it is developed using OrmoDev for 2 mins followed by a bath with isopropanol and drying using pressurized air. Figure 2(b), shows a part of a fabricated binary grating on electronic photoresist, whereas Figs. 2(a, c, and d) show the structures on grayscale photoresist. One can also create the waveguide structures on the electronic resist, for which the spinning speed should be much slower to obtain a thick layer of resist of 10 µm. But for slower spinning speed, an inhomogeneous layer thickness emerges across the sample surface. To circumvent this, the single waveguide structures are also fabricated on grayscale photoresist. For creating longer waveguides, as required for realistic applications multiple single waveguide patterns are stitched together. Any geometry of planar waveguides is possible by

OSA CONTINUUM

stitching of single patterns, see Fig. 3(a). For stitching of single patterns, typically a stitching error occurs in the fabricated structures. This error appears in the form of a displacement from the ideal position while moving the translation stage as illustrated in Fig. 3(b). The measured stitching error without any compensation is around 3 µm, which can be minimized by using a software GUI (Graphical User Interface) in MATLAB. After compensation of the displacement error, a residual stitching is still visible, Fig. 3(c), which is less than 1 µm. The depth profile of the replicated waveguide obtained using confocal microscopy is shown in Fig. 3(d).

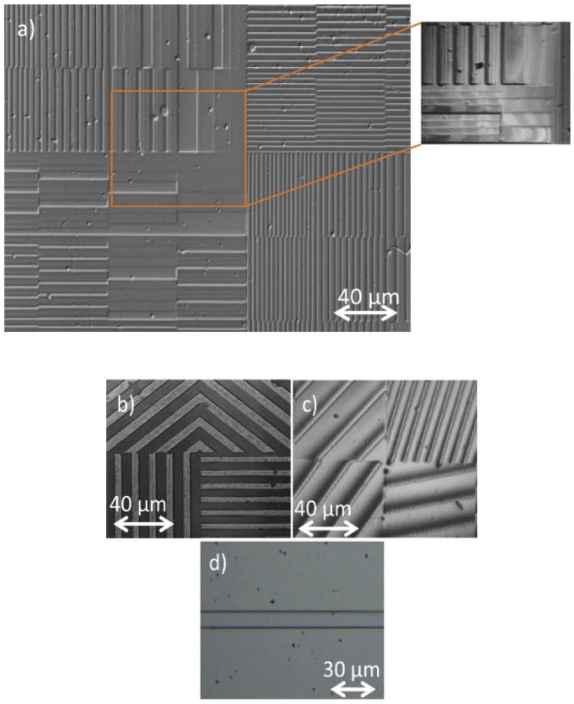

Fig. 2. Fabricated grating and waveguide microstructures (a) Large section of four level gratings with varying periods on gray scale resist, (b) binary gratings on binary resist, (c) multilevel sawtooth gratings on gray scale resist, and (d) multimode waveguide structure on grayscale resist.

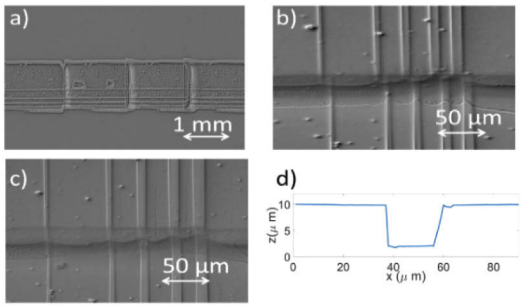

Fig. 3. Fabricated stitched waveguides (a) Stitching single patterns together forming long waveguide, (b) stitched patterns showing large stitching errors, (c) stitched patterns with minimal stitching error, (d) depth profile of the replicated waveguide structures measured with confocal microscopy.

OSA CONTINUUM

The next step in our process chain is to replicate the desired structures on polymer [e.g. PMMA]. To do this, a lab-made hot embossing system is employed. It consists of two heating plates and a force unit. The sample is placed inside the heating plates and after reaching the embossing temperature, the desired amount of force is applied to replicate the structures [18]. Prior to this step, the grating or waveguide structures on the wafer are converted into a polydimethylsiloxane (PDMS) stamp which is used for soft replication on PMMA. This is because the fabricated structures are not able to withstand the high thermal loads required for embossing. The intermediate stamp is made by using PDMS casting. For the embossing process, a homogenous PDMS stamp is necessary to replicate the grating structures. In our simple, lab-made hot embossing system, there might be some misalignment between the two heating plates. To compensate this, an embossing approach is used, where an additional blank PDMS stamp is placed on bottom of the sample to distribute the applied force homogenously over the sample area, see Fig. 4(a). The PDMS stamp is then placed in the self-made hot embossing machine and a sheet of PMMA with a thickness of 500 µm is positioned on top of the stamp. Both elements are heated to an embossing temperature which in our case is 140 °C, well above the glass transition temperature of PMMA, i.e. 105 °C, and an embossing force of 7KN is applied, as indicated in Fig. 4(a). Then the elements are demolded at a temperature of 60 °C. The whole process for replication on polymer is described in [10].

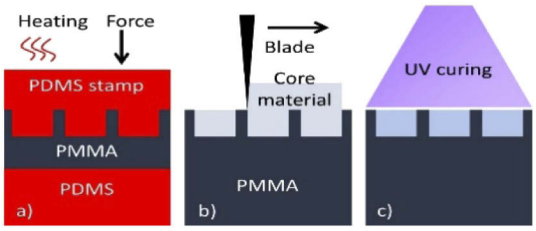

Fig. 4. Method for hot embossing soft replication process. (a) Hot embossing process, (b) waveguide filling with core material and blading, and (c) UV flood exposure and curing of the structure.

Gratings and waveguide structures are replicated in the same way: the basic structure is imprinted into the polymer. In case of the waveguides, the structure is then filled with the UV curable core material. The core material used in this work is NOA-68 (Norland Inc.) with a refractive index R. I. ≈ 1.54 of the cured polymer. Initially, the core material is in liquid form which solidifies upon curing by UV light. After application onto the waveguide structure the excessive material is removed by a blading process, as indicated in Fig. 4(b). The waveguide filled with the core material is then exposed to UV light with a wavelength of 365 nm for 20 mins to solidify and a perpendicular cut is applied using a weighted mechanical razor tool to create smooth end facets with much smaller surface roughness compared to the wavelength of the incoming light, see Fig. 4(c).

4. Characterization of the optical structures

The fabricated grating structures are characterized by measuring the period height profiles and the transmission and diffraction efficiencies. The grating profile determines the diffraction pattern and the diffraction efficiency in a certain diffraction order. Also, it is related to the illumination source wavelength. For application in automotive industry, for example, for rear end lamps, we have selected a wavelength of 632 nm which is in accordance with the regulations defined by the European commission (ECE) [19]. For binary grating structures, the desired height profile is 316 nm considering the thin element approximation as in [20]. This can be achieved by suitable spin coating of the photoresist on the wafer surface. We have achieved a profile height of 340 nm

OSA CONTINUUM

which is in close agreement with the desired value. The structures on the silicon wafer are then transferred to the polymer (PMMA), using the hot embossing system as discussed earlier. The replicated grating structure height profile measured using the confocal microscope can be seen in Fig. 5(a). For multilevel structures Ormocomp resist is used. For a grating structure exhibiting four height levels, a height difference of approx. 160 nm between two of the levels is desired. This value depends on the illumination wavelength the structure is designed for (which is 632 nm in this case). The structure is exposed to the modulated UV light and after the developing process (as described above) it is also replicated. Typical height profiles of grating structures with four height levels are displayed in Fig. 5(b).

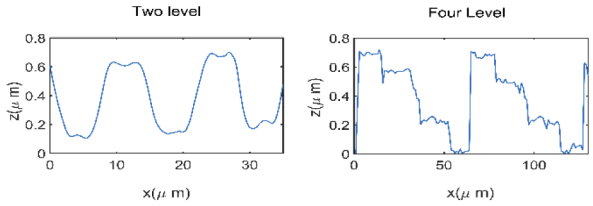

Fig. 5. Typical surface height profiles of replicated grating structures measured using confocal microscopy. (a) Binary gratings having a period of 10 µm and height of 340 nm, (b) four-level gratings having a period of 60 µm and height of 680 nm.

Periods of 10 µm and 60 µm are measured using confocal microscopy for binary gratings and four-level gratings, respectively. For binary structures, one can fabricate smaller structure periods down to 1.3 µm with the employed optical system and a 10x objective lens. By increasing the magnification of the objective lens, fabrication of submicron structures is possible. Similarly, for multilevel structures smaller periods are achievable but also process complexity is increased. A further way to characterize the fabricated grating structures is to measure the diffraction of the incident light in a certain diffraction order. The diffraction efficiency depends on the structure and the material used. For grating structures on PMMA, the diffraction in the first diffraction order is measured by illumination with a He-Ne laser at a wavelength of around 632 nm. The total power from the laser measured using a power meter (Thorlabs S121C) is P_{Total}=1.57 mW. The measured diffracted power of the first order of the binary grating is $P_{binary} = 650$ µW, which gives a diffraction efficiency of $\eta_{binary} = 41.4\%$. Similarly, for the four-level grating structure the measured power of the first diffraction order is $P_{multi} = 1.13$ mW, yielding a diffraction efficiency of $\eta_{multi} = 71.9\%$. An increase in the diffraction efficiency is observed when using four-level gratings in comparison to binary gratings. The diffraction efficiency can also be theoretically estimated by simulating the design given the period, height, material (refractive index) and the geometry of the grating structures using rigorous coupled wave analysis (RCWA) [21,22]. The simulated diffraction efficiency for our case is 44% and 76.5% for binary gratings and four-level gratings, respectively. The diffraction pattern resulting from the illumination of the fabricated binary gratings is seen in Fig. 6(a). An intense center spot which is the zero-diffraction order (or non-diffracted light) dominates over the first diffraction order, see Fig. 6(a). On the other hand, a much brighter first order diffraction pattern is observed for the four-level gratings, see Fig. 6(b).

The multimode waveguide structures are characterized in terms of propagation losses. The measurement method used for propagation losses is based on the destructive cut-back method [23]. The investigation is conducted at a wavelength of 638 nm from a fiber coupled laser diode (MCLS1-638, Thorlabs). The output power is measured using a fiber coupled photodiode sensor (S152C, Thorlabs). Using a three-axis precision stage, the input and output fibers are positioned precisely. The total processible area of the SLM screen is 1.53 mm x 0.86 mm, however, because of a field stopper used to remove the border of the SLM screen, an effective area of 1.2 mm x 0.6 mm is accessible. The length of the waveguides fabricated is 2.4 cm and a total of twenty

OSA CONTINUUM

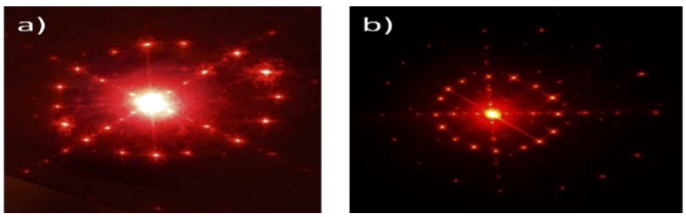

Fig. 6. Resulting illumination pattern. (a) Binary gratings, (b) four-level gratings showing higher diffraction orders.

single patterns are stitched together with each single pattern having a length of 1.2 mm. The beam spot at the input fiber is approx. 0.50 mm^2 and the waveguide channel width and depth are 20 µm and 8 µm, respectively. The output power from the source is 0.6 mW, measured at the input facet of the waveguide. The output power measured at the end facet at a length of 2.2 cm is 0.152 mW. For characterization, length cuts are applied at 1.1 cm, 0.8 cm and 0.4 cm, and the transmitted power measured is 0.243 mW, 0.355 mW and 0.425 mW, respectively. The coupling of input light into the waveguide is seen in Fig. 7(a), and the observed optical power (in dBm) with different waveguide lengths in Fig. 7(b). The measured insertion loss (IL) is 1.13dB. The graph shows an increase in output power as the length of the waveguide is shortened. The output power loss in the waveguide is described by the attenuation in the fiber as well as losses at the intersecting facets of the individual stitched patterns. The average propagation loss measured using the cut-back method is 2.07dB/cm at a wavelength of 638 nm. This loss level is still acceptable in view of the fact that the stitching process for the realization of the waveguide cladding structure is associated with a positioning error (less than 1 µm currently, see Fig. 3) which leads to optical losses at the interface between stitched segments. Also, the optical performance is sufficient for future application for integrated sensing and might still be improved by optimization of the manufacturing process. As for the repeatability of the experiment, for each iteration, considering multiple processes from fabrication and replication to measurement setups, one can expect smaller changes approx. less than 5% in the values of diffraction efficiencies, propagation, and insertion losses, respectively.

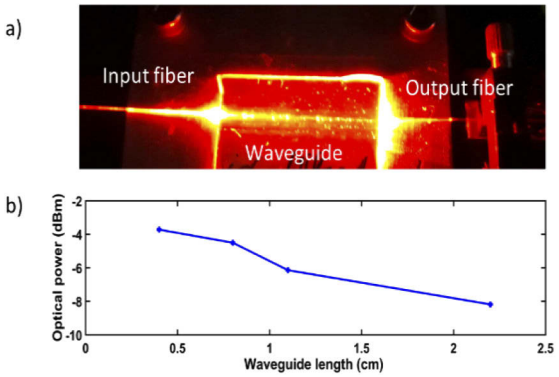

Fig. 7. Characterization of fabricated waveguides. (a) Image of the light transmission path in the waveguide, (b) optical power (in dBm) as function of length of the waveguide measured using the cut-back method.

OSA CONTINUUM

5. Conclusion

The method and optical system presented in this work to create polymer micro- and tentatively nanostructures, i.e. binary and multilevel gratings as well as multimode waveguides, provides flexibility for producing even smaller (submicron) structures by using higher de-magnification lenses. In general, the employed optical system enables the production of versatile structures. Also, the speed of fabrication can be increased by stitching of single exposure patterns, as demonstrated in a proof-of-principle. We have also shown that the material used for multilevel structures can be employed to create binary structures as well, but the processing time of the resist is longer compared to the electronic resist. For binary gratings, multilevel gratings and waveguide structures, the self-made hot embossing system can faithfully be used for replication without distorting the shape profile too much. The binary gratings show an intense zero-order diffraction spot upon illumination with a He-Ne laser compared to the four-level gratings where the diffractive intensity in the first order is increased almost 1.5 times. By increasing the number of levels, diffraction in the first order can further be increased. However, replication on polymer, e.g. PMMA using hot embossing will be more difficult in that case and other methods such as injection molding might be more suitable [24]. The diffractive grating structures with minimum zero-order diffraction pattern can be employed to project information in automotive rear end lights as indicated in [6]. Furthermore, the fabricated waveguide and grating structures might be used for applications in integrated photonics i.e. sensing and optical interconnects [25–27] which is also intended in our next steps.

Funding

Deutsche Forschungsgemeinschaft (EXC 2122, Project ID 390833453, PhoenixD); Niedersächsisches Ministerium für Wissenschaft und Kultur (Tailored Light).

Acknowledgments

The publication of this article was funded by the Open Access Fund of the Leibniz Universität Hannover.

Disclosures

The authors declare no conflicts of interest.

References

1. M. Rezem, A. Günther, B. Roth, E. Reithmeier, and M. Rahlves, "Low-Cost Fabrication of All-Polymer Components for Integrated Photonics," J. Lightwave Technol. **35**(2), 299–308 (2017).
2. A. Günther, A. B. Petermann, U. Gleissner, T. Hanemann, E. Reithmeier, M. Rahlves, M. Meinhardt-Wollweber, U. Morgner, and B. Roth, "Cladded self-written multimode step-index waveguides using a one-polymer approach," Opt. Lett. **40**(8), 1830–1833 (2015).
3. C. Kelb, M. Rahlves, E. Reithmeier, and B. Roth, "Realization and Performance of an All-Polymer Optical Planar Deformation Sensor," IEEE Sens. J. **15**(12), 7029–7035 (2015).
4. C. Kelb, R. Rother, A. K. Schuler, M. Hinkelmann, M. Rahlves, O. Prucker, C. Müller, J. Rühe, E. Reithmeier, and B. Roth, "Manufacturing of embedded multimode waveguides by reactive lamination of cyclic olefin polymer and polymethylmethacrylate," Opt. Eng. **55**(3), 037103 (2016).
5. H. Ma, A. K.-Y. Jen, and L. R. Dalton, "Polymer-based optical waveguides: Materials, processing, and devices," Adv. Mater. **14**(19), 1339–1365 (2002).
6. M. S. Khan, M. Rahlves, R. Lachmayer, and B. Roth, "Polymer-based diffractive optical elements for rear end automotive applications: design and fabrication process," Appl. Opt. **57**(30), 9106–9113 (2018).
7. M. Rezem, C. Kelb, A. Günther, M. Rahlves, E. Reithmeier, and B. Roth, "Low-cost fabrication of optical waveguides, interconnects and sensing structures on all-polymer-based thin foils," Proc. SPIE **9751**, 975112 (2016).
8. P. van Assenbergh, E. Meinders, J. Geraedts, and D. Dodou, "Nanostructure and Microstructure Fabrication: From Desired Properties to Suitable Processes," Small **14**(30), 1801989 (2018).
9. M. T. Gale, M. Rossi, J. Pedersen, and H. Schutz, "Fabrication of continuous-relief micro-optical elements by direct laser writing in photoresists," Opt. Eng. **33**(11), 3556–3566 (1994).

OSA CONTINUUM

10. M. Rahlves, M. Rezem, K. Boroz, S. Schlangen, E. Reithmeier, and B. Roth, "Flexible, fast, and low-cost production process for polymer based diffractive optics," Opt. Express **23**(3), 3614–3622 (2015).
11. M. Rahlves, C. Kelb, M. Rezem, S. Schlangen, K. Boroz, D. Gödeke, M. Ihme, and B. Roth, "Digital mirror devices and liquid crystal displays in maskless lithography for fabrication of polymer-based holographic structures," J. Micro/Nanolithogr., MEMS, MOEMS **14**(4), 041302 (2015).
12. J. Kanti, T. J. Dunn, and J. M. Hoffman, "Seamless, maskless lithography system using spatial light modulator," U.S. Patent No. 6,312,134 (2001).
13. K. F. Chan, Z. Feng, R. Yang, A. Ishikawa, and W. Mei, "High-resolution maskless lithography," J. Micro/Nanolithogr., MEMS, MOEMS **2**(4), 331–340 (2003).
14. L. Pan, Y. Park, Y. Xiong, E. Ulin-Avila, Y. Wang, L. Zeng, S. Xiong, J. Rho, C. Sun, D. B. Bogy, and X. Zhang, "Maskless Plasmonic Lithography at 22 nm Resolution," Sci. Rep. **1**(1), 175 (2011).
15. L. Ningning and Z. Zhang, "Fabrication of a curved microlens array using double gray-scale digital maskless lithography," J. Micromech. Microeng. **27**(3), 035015 (2017).
16. Q. Zheng, J. Zhou, Q. Chen, L. Lei, K. Wen, and Y. Hu, "Rapid Prototyping of a Dammann Grating in DMD-Based Maskless Lithography," IEEE Photonics J. **11**(6), 1–10 (2019).
17. F. A. W. Coumans, E. van der Pol, and L. W. M. M. Terstappen, "Flat-top illumination profile in an epifluorescence microscope by dual microlens arrays," Cytometry **81A**(4), 324–331 (2012).
18. C.-W. Tsao, "Polymer Microfluidics: Simple, Low-Cost Fabrication Process Bridging Academic Lab Research to Commercialized Production," Micromachines **7**(12), 225 (2016).
19. Economic Commission of Europe, "Einheitliche Bedingungen für die Genehmigung von Fahrzeugen hinsichtlich des Anbaus der Beleuchtungs- und Lichtsignaleinrichtungen," *Regelung Nr.* 48, (2016).
20. F. B. McCormick, "Generation of large spot arrays from a single laser beam by multiple imaging with binary phase gratings," Opt. Eng. **28**(4), 284–299 (1989).
21. M. G. Moharam, E. B. Grann, D. A. Pommet, and T. K. Gaylord, "Formulation for stable and efficient implementation of the rigorous coupled-wave analysis of binary gratings," J. Opt. Soc. Am. A **12**(5), 1068–1076 (1995).
22. M. G. Moharam, D. A. Pommet, E. B. Grann, and T. K. Gaylord, "Stable implementation of the rigorous coupled-wave analysis for surface-relief gratings: enhanced transmittance matrix approach," J. Opt. Soc. Am. A **12**(5), 1077–1086 (1995).
23. R. Ramponi, R. Osellame, and M. Marangoni, "Two straightforward methods for the measurement of optical losses in planar waveguides," Rev. Sci. Instrum. **73**(3), 1117–1120 (2002).
24. C. Yang, X. H. Yin, and G. M. Cheng, ""Microinjection molding of microsystem components: new aspects in improving performance,"," J. Micromech. Microeng. **23**(9), 093001 (2013).
25. M. Rahlves, A. Günther, M. Rezem, and B. Roth, "Polymer-Based Transmission Path for Communication and Sensing Applications," J. Lightwave Technol. **37**(3), 729–735 (2019).
26. M. Suar, O. Melchert, M. Rahlves, and B. Roth, "Experimental and theoretical study of the formation process of photopolymer based self-written waveguides," Opt. Express **27**(26), 38326–38336 (2019).
27. L. Zheng, U. Zywietz, A. Evlyukhin, B. Roth, L. Overmeyer, and C. Reinhardt, "Experimental Demonstration of Surface Plasmon Polaritons Reflection and Transmission Effects," Sensors **19**(21), 4633 (2019).